# Numerical study of sediment particle trajectories under tidal bores

**Y. Satria Putra[a], A. Beaudoin, M. Ramos Ortega, G. Rousseaux and S. Huberson**

a. Institute of Pprime, Téléport 2, Boulevard Marie et Pierre Curie, BP 30179, 86962 Futuroscope Chasseneuil Cedex France + email yoga.satria.putra@univ-poitiers.fr

## Abstract :

*The tidal bores occur in the shallow mouths of some rivers when high tides rise in the narrow funnel-shaped estuaries. There are two types of tidal bores. Low Froude numbers $Fr$ lead to low turbulences in the river flows, inducing undular tidal bores. High Froude numbers $Fr$ lead to high turbulences in the river flows, inducing breaking tidal bores. The study of sediment particle trajectories under tidal bores will help to understand the mechanisms of sediment transport in the river flows where the tidal bore phenomenon can appear. OpenFOAM, a CFD code, was used to simulate undular and breaking tidal bores by varying the Froude number $Fr$ between 0.99 and 1.66. The validation of numerical simulations was performed by means of Lemoine's theory. The analysis of wave amplitude $a_w$ and wavelength $L_w$ has allowed to define the transition between the hydraulic jump and the undular tidal bore, and the transition between the undular and breaking tidal bores. $L_w$ approaches the infinity when the undular tidal bore becomes a hydraulic jump. The decrease of wave amplitude $a_w$ is related to the presence of breaking tidal bores. The undular tidal bore appears for $Fr_1 > 1.04$. It becomes partially breaking for $Fr_2 > 1.43$ and totally breaking for $Fr_3 > 1.57$. A tracker method, based on solving of Maxey-Riley equations, was used to estimate the trajectory of sediment particles under tidal bores. The analysis of sediment particle trajectories was performed by means of modified Chen's model. The modications of Chen's model use three parameters denoted by $\beta_1$, $\beta_2$ and $\beta_3$. The relation between each parameter and the Froude number $Fr$ was established. $\beta_1$, related to the front celerity, decreases when $Fr$ increases. The undular tidal bores move faster than the breaking tidal bores. $\beta_2$ and $\beta_3$, related to the elevation and the attenuation, increase when $Fr$ increases. The train of undulations disappears with $Fr$. The wave breaking is responsible of the disappearance of undulations.*

**Keywords : Sediment transport, Maxey-Riley equations, tracker method, tidal bore, Froude number, OpenFoam.**

## Introduction

The tidal bore is a natural phenomenon in the estuaries having a convergent river mouth like an uterine section shape with a low slope (Fig. 1). A tidal bore is formed during a spring tide when the tidal range exceeds 5 $m$ to 6 $m$ in a narrow funnel-shaped estuary according to Chanson [4]. The propagation direction of the tidal bore wave is opposite to the river current. The positive surge propagates upstream the river. The tidal bores occur in many locations in the world. Its name may vary from one country to another. This phenomenon is called *Pororoca* on the Amazon River in Brazil, *Burro* on the Colorado River in Mexico, *Benak* on the Batang Lupar River in Malaysia, *Aegir* on the Trent River in the United Kingdom, *Silver Dragon* on the Qiantang River in China, *Mascaret* on the Garonne River in France and *Bono* on the Kampar River in Indonesia [2].

In the literature, some works were realized to define the transition between the tidal jump and the undular tidal bore, and the transition between the undular and breaking tidal bores. A study was done by Furgerot [7] who classified the tidal bores with the Froude number $Fr$. She observed the two transitions. In their works, Khezri [10] and Simon [13] generated experimentally and numerically the two types of tidal bores, undular and breaking, for Froude numbers $Fr$ ranging from 1 to 1.36. They used the CFD software Thétis to generate the numerical simulations. Khezri estimated the wave amplitude $a_w$ and the wavelength $L_w$ from the form of free surface. Simon studied the hydrodynamics of tidal bores from flow velocity fields. However the question of the definition of both transitions is always topical.

During the passage of a tidal bore, sediment particles are eroded, transported and deposited in the river. The sediment particles are also dispersed in a turbulent flow due to a collision between two currents in opposite directions, upstream (river flow) and downstream (tidal bore). Recent works were performed for understanding the influence of tidal bores on the sediment transport. The dispersion of fish eggs induced by tidal bores was observed by Chanson [4]. The experimental trajectory of fish eggs looks like the theoretical trajectory given by Chen [5]. This theoretical trajectory has been obtained with the wave - current theory. In his thesis, Berchet [1] developed a tracker model based on solving the Maxey-Riley equations to estimate the trajectory of sediment particles under tidal bores. From numerical simulations of undular tidal bores, obtained with the CFD software Thétis, he obtained numerical trajectories similar to those given by the wave - current theory. Then, a complete comparison between the experimental or numerical trajectories and the theoretical trajectories of Chen's model is possible.

In this work, there are two main objectives. The first objective is to define the limit values of Froude number $Fr$ between the hydraulic jump, the undular tidal and breaking tidal bores, by estimating the wave amplitude $a_w$ and the wavelength $L_w$ from numerical simulations obtained with the CFD software OpenFOAM. The configuration used by Khezri [10] and Simon [13] is considered here to obtain the free surface and the flow velocity field. The values of wave amplitude $a_w$ and wavelength $L_w$ are validated by using the Lemoine's theory. The second objective is to modify the Chen's model by analyzing the sediment particle trajectories obtained in the case of undular tidal bores with a tracker model based on solving the Maxey-Riley equations [1]. The Chen's model doesn't consider the sedimentation induced by the gravity. When a tidal bore moves in the river, two modifications of sediment particle trajectories appear, elevation and attenuation. Three parameters, denoted $\beta_1$, $\beta_2$ and $\beta_3$, are introduced into the Chen's model in order to take into account these process. A parametric study allows to establish the relation between each parameter and the Froude number $Fr$.


(a) (b)

FIGURE 1 – (a) Undular tidal bore on the Kampar river in Indonesia (https://www.youtube.com/watch?v=Yn_A2HiamgU) and (b) Breaking tidal bore on the Qiantang River in China (photographed by Chanson [10]).

# Numerical and theoretical tools

In this section, we explain the different tools used in this paper. Firstly, we describe how to generate the numerical simulations of tidal bore flows with OpenFOAM. Secondly, we explain the tracker method used to estimate the particle trajectories in rivers under tidal bores. Thirdly, we present an adimensional parameter used to classify the tidal bores. Fourthly, we describe the Lemoine's theory used to analyse the tidal bore flows. Finally, we discuss the modified Chen's model used to analyse the trajectory of sediment particles in rivers under undular tidal bores.

# Tidal bore flows

The 2D numerical simulations of tidal bore flows were obtained with the CFD software OpenFOAM (Open source Field Operation And Manipulation) based on solving Navier-Stokes equations :

$$\nabla \cdot \mathbf{u} = 0 \quad \text{and} \quad \rho \left( \frac{\partial \mathbf{u}}{\partial t} + (\mathbf{u} \cdot \nabla)\mathbf{u} \right) = \rho \mathbf{g} - \nabla p + \nabla \cdot \left[ \mu (\nabla \mathbf{u} + \nabla^T \mathbf{u}) \right] \tag{1}$$

where $\mathbf{u}$ is the flow velocity, $t$ is the time, $p$ is the total pressure, $\mathbf{g}$ is the gravity, $\rho$ is the fluid density and $\mu$ is the dynamic viscosity of the fluid. The flow of two incompressible fluids, water and air, is considered here. The density and viscosity of water ($w$) and air ($a$) are $\rho_w$ = 1000 $kg/m^3$, $\rho_a$ = 1.1768 $kg/m^3$, $\mu_w$ = $10^{-3}$ $kg/ms$ and $\mu_a$ = $1.85 \times 10^{-5}$ $kg/ms$. The initial flow velocity of water $U_1$ is taken from the laboratory conditions of Kehzri's thesis [10]. For the two most breaking configurations, $U_1$ is equal either to 0.8 $m/s$ or 0.9 $m/s$. A tidal bore is numercially generated by simulating the impact of an initial current on a gate blocking the open channel. Then, the water level increases quickly followed by a reflection opposited to the current, the run up. The gate can be completely or partially close to generate a breaking or undular tidal bore with the same initial flow conditions (Fig. 2). The gate is located at the abscissa $x$ = 0 $m$. The gate opening $h_g$ ranges from 0 $mm$ to 135 $mm$. The initial water depth $d_o$ is fixed to 0.14 $m$. The 2D numerical simulations were stopped at a time $t$ ranging from 10 $s$ to 15 $s$, depending on the considered configuration of the gate closing.

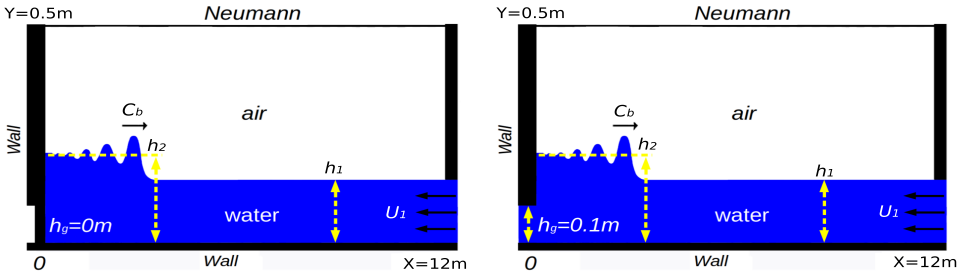


FIGURE 2 – Sketch of the physical domain used for the numerical simulations of tidal bores, (a) fully closed gate ($hi_g$ = 0 $m$) and (b) partially closed gate ($h_g \neq 0$ $m$).

The Finite Volume method is used to discretize the Navier-Stokes equations on a regular grid of dimensions 12 $m \times 0.5$ $m$. The computational grid is composed of two or three blocks in function of the gate closing. The first block corresponds to the flow zone under the gate, the second block to the flow zone between the first block and the free surface, and the third block to the air phase. In the two directions, parallel ($x$) and perpendicular ($y$) to the flow direction, the number of cells is 2400 and 120 respectively. The total pressure $P$ is estimated at the vertice of cells. The components of the flow velocity $\mathbf{u}$ are obtained on the side of cells (Fig. 3). The Navier-Stokes equations are integrated on each control volume and discretised in terms of physical fluxes through the control volume faces [13].

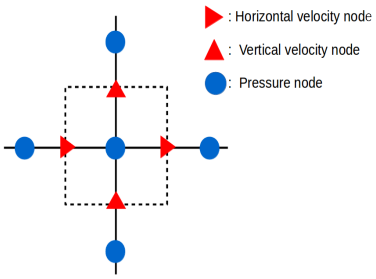


FIGURE 3 – Mesh and control volume for a staggered grid.

# Sediment transport

A tracker model has been developed during the Phd thesis by Berchet [1] to study the sediment transport under a tidal bore. This numerical model is based on the estimation of sediment particle trajectories by solving the Maxey-Riley equations. These equations describe the trajectory of one spherical particle in a fluid flow :

$$\frac{d\mathbf{X}_i}{dt} = \mathbf{V}_i(\mathbf{X}_i, t) \quad \text{and} \quad m_i \frac{d\mathbf{V}_i}{dt} = \sum_j \mathbf{F}_j(\mathbf{X}_i, t) \tag{2}$$

where $\mathbf{X}_i$ is the location of the sediment particle $i$, $\mathbf{V}_i$ is the velocity of the sediment particle $i$, $m_i$ is the mass of the sediment particle $i$ and $\mathbf{F}_j$ is a force acting on the sediment particle $i$. The force of gravity, the force of pressure gradient around the grain, the force of added mass, the viscous drag and the Basset force are considered here [1] :

$$\begin{aligned} \frac{d\mathbf{V}_i}{dt} &= 2\frac{\rho_p - \rho_f}{2\rho_p + \rho_f}\mathbf{g} + \frac{3\rho_f}{2\rho_p + \rho_f}\frac{D\mathbf{u}_i}{Dt} - \frac{3}{4r_i}\frac{\rho_f}{2\rho_p + \rho_f}(\mathbf{V}_i - \mathbf{u}_f)||\mathbf{V}_i - \mathbf{u}_f||C_D \\ &- \frac{9}{2r_i}\frac{\rho_f}{\rho_p + \frac{\rho_f}{2}}\sqrt{\frac{\nu}{\pi}}\int_0^t \frac{d(\mathbf{V}_i(\tau) - \mathbf{u}_i(\tau))}{d\tau}d\tau\frac{d\tau}{\sqrt{(t-\tau)}} \end{aligned} \tag{3}$$

where $r_i$ is the radius of the sediment particle $i$, $\rho_p$ and $\rho_f$ are the densities of sediment particles and the fluid, $\nu$ is the kinematic viscosity of the fluid and $C_D$ is the drag coefficient. The radius and density of sediment particles are $r_i$ = 100 $m$ and $\rho_p$ = 1000 $kg/m^3$ respectively. The time discretization of the previous system of equations uses the fourth order Runge-Kutta scheme. To obtain the trajectory of sediment particles, it is necessary to have the flow velocity field during the passage of tidal bores. The flow velocity field is estimated with OpenFOAM presented in the previous section.

# Froude number

Generally, the strength and shape of tidal bores are linked to the Froude number $Fr$. In the work by Furgerot [7], Table 1 is given to establish a classification of tidal bores with the Froude number $Fr$. The large Froude number, $Fr > 1.52$, will lead to high turbulence in the river flow. Then, a breaking tidal bore will appear. The small Froude number, $Fr < 1.52$, will bring up a low turbulence in the river flow. Then, an undular tidal bore will appear. The Froude number $Fr$ depends on the initial flow velocity $V_0$ and the water height $d_0$ in the upstream part of the river, and also the bore velocity $U_b$ (positive downstream) [10] :

$$Fr = \frac{U_1 + C_b}{\sqrt{gh_1}}. \tag{4}$$

According to Table 1, we can see that the tidal jump is not always a tidal bore. To be a tidal bore, it has to be visible with a flood bar crossing the river transversally.

TABLE 1 – Classification of tidal bores with the Froude number $Fr$ given by Furgerot [7].

| Froude number | Bore observation |
|---|---|
| $Fr < 1$ | No tidal bore |
| $1 < Fr < Fr_c$ | Low frequency wave |
| $Fr_c < Fr < 1.2$ to $1.25$ | Generate shock wave |
| $1.25 < Fr < 1.47$ | Undular tidal bore |
| $1.47 < Fr < 1.52$ | Transient tidal bore |
| $Fr > 1.52$ | Breaking tidal bore |

# Lemoine's theory

Using the approximation of linear wave theory, Lemoine developed analytical expressions giving the wave amplitude $a_w$ and the wavelength $L_w$ [14] :

$$\frac{a_w}{h_2} = \left(\frac{h_2 - h_1}{h_2}\right)\left(\frac{h_2 - h_1}{h_1}\right)^{1/2}\left(1 - \frac{2kh_2}{\sinh(2kh_2)}\right)^{-1/2} \tag{5}$$

$$\frac{L_w}{h_2} = \pi\frac{h_1}{h_2}\left(1 + \frac{h_1}{h_2}\right)\tanh^{-1}\left(2\pi\frac{h_2}{L_w}\right) \tag{6}$$

where each term of these equations corresponds to a variable shown in Figure 4. $k = \frac{2\pi}{L_w}$ is the quantity of undulations. These equations are validated in the case where the whelps have the same front celerity. When the Froude number $Fr$ is almost 1 and the tidal bore passage is in a very shallow water $h_2/L_w \ll 1$, the previous equations can be simplified :

$$\frac{a_w}{h_2} \sim \frac{1}{\sqrt{3}}\left(\frac{h_2 - h_1}{h_1}\right) \quad \text{and} \quad \frac{L_w}{h_2} \sim 2\pi\sqrt{\frac{2}{3}}\left(\frac{h_2 - h_1}{h_1}\right)^{-1/2}. \tag{7}$$

These equations show that the whelps are characterized by the tidal bore intensity $I_r = (h_2 - h_1)/h_1$. Whatever the type of the tidal bore, undular or breaking, its hydrodynamics will be controlled by two adimensional parameters, the tidal bore intensity $I_r$ and the Froude number $Fr$.

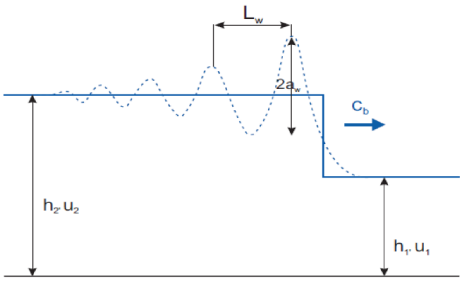


FIGURE 4 – Sketch of a hydraulic jump and variables used in the Lemoine's theory [14].

# Chen's model

In this work, we propose three modifications of Chen's model to obtain an analytical solution allowing to analyse the sediment particle trajectories under undular tidal bores. This objective is reached by decomposing the sediment particle trajectories into three contributions [1] :

1. *Gravity* : Considering a constant settling velocity $w_s$, the contribution of gravity in the sediment particle trajectories is given by :

$$y(t) = -w_s(t - t_0) \tag{8}$$

where $t_0$ is the initial time of sediment particle trajectories.

2. *Elevation* : During the passage of an undular tidal bore, an elevation of the free surface appears simultaneously to a slowing down of the river current. Their effects on the sediment particle trajectories can be collected in the same equation in which the water height changes from $h_1$ to $h_2$ and the current velocity changes from $U_1$ to $U_2$ :

$$x(t) = \frac{1}{2\beta_1}((U_1 - U_2)\log(\cosh(-\beta_1)t_B) - \log(\cosh(\beta_1(t - t_B)))) + \beta_1(U_1 + U_2)t \quad (9)$$

$$y(t) = \frac{h_2 - h_1}{2}\tanh(\beta_2(t - t_B)) \quad (10)$$

where $t_B$ is the time taken by the sediment particles to go through the jump front, $\beta_1$ is the parameter controlling the flow velocity during the slowing down between the two states before and after the front, and $\beta_2$ is the parameter controlling the velocity of elevation between the two states.

3. *Attenuation* : The secondary waves amplitude decreases with the distance. It is probably that the attenuation is a combination of dispersive and dissipative effects to be elucidated. This effect on the sediment particle trajectories can be described by :

$$x(t) = x_{chen}(t)\exp(-\beta_3(t)) \quad (11)$$

$$y(t) = y_{chen}(t)\exp(-\beta_3(t)) \quad (12)$$

where $\beta_3$ is the attenuation parameter and $(x_{chen}, y_{chen})$ are the solutions proposed by Chen [5].

# Numerical results

## Flow analysis

The numerical results of tidal bores obtained with OpenFOAM are compared to the analytical results obtained with the Lemoine's theory. The numerical values of wave amplitude $a_w$ and wavelength $L_w$ are given by the equations following :

$$a_w = \frac{Y_1 - Y_{min}}{2} \quad \text{and} \quad L_w = X_1 - X_2. \quad (13)$$

$Y_1$ and $X_1$ are associated to the front elevation. $Y_2$ and $X_2$ are associated to the first whelp elevation. $Y_{min}$ is the lowest height between the front and the first whelp. All these quantities are shown in Figure 5. In the case of breaking tidal bores, the average values of firsts undulations are taken. Table 2 gives the numerical values of $a_w$ and $L_w$ for Froude numbers $Fr$ ranging from 0.99 to 1.66.

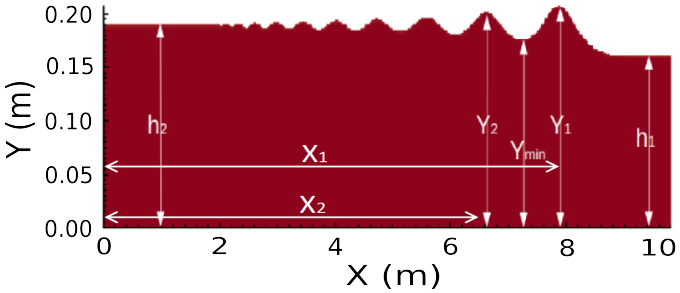


FIGURE 5 – Definition of variables $Y_1$, $Y_2$, $X_1$, $X_2$ and $Y_{min}$ used in the equation 13 for the estimation of wave amplitude $a_w$ and wavelength $L_w$.

Figures 6, 7 and 8 show the adimensional values of $Y_{min}/h1$, $L_w/h1$ and $a_w/h1$ as functions of Froude

number $Fr$. The theoretical results are given by Lemoine [14] and Tissier [14], the experimental results are given by Favre [6] and Treske [15], and the numerical results are obtained by using OpenFOAM. In Figure 6, the agreement between the different results is correct. The comparison of different results, theoretical, experimental and numerical, allows to validate the numerical simulations obtained with OpenFOAM. In Figure 7, the numerical results obtained with OpenFOAM have the same behavior than those given by the Lemoine's theory (simplified or complete). The adimensional values of $L_w/h1$ decrease when $Fr$ increases. This decrease is induced by the flood of breaking tidal bores. Figure 7 shows that a tidal jump becomes an undular tidal bore for $Fr = 1.04$ because a tidal jump gives a infinity value of $L_w/h1$. Figure 8 allows to find the transition between a total undular tidal bore and a partial breaking tidal bore ($Fr_2$ = 1.43), and the transition between a partial breaking tidal bore and a total breaking tidal bore ($Fr_3$ = 1.57).

TABLE 2 – Numerical values of wave amplitude $a_w$ and wavelength $L_w$, measured from visualizations obtained with the software Paraview.

| **Test** | $h_1$ $(m)$ | $hg$ $(m)$ | $Fr$ | $X_1$ $(m)$ | $Y_1$ $(m)$ | $X_2$ $(m)$ | $Y_2$ $(m)$ | $Y_{min}$ $(m)$ | $a_w$ | $L_w$ | $I_r$ |
|---|---|---|---|---|---|---|---|---|---|---|---|
| 1 | 0.14 | 0.135 | 0.994 | 3.2 | 0.1456 | 1.7 | 0.143 | 0.142 | 0.0018 | 1.5 | 0 |
| 2 | 0.14 | 0.13 | 1.041 | 3.4 | 0.153 | 2 | 0.15 | 0.146 | 0.0035 | 1.4 | 0.04 |
| 3 | 0.14 | 0.12 | 1.109 | 4.11 | 0.174 | 2.88 | 0.1666 | 0.151 | 0.0115 | 1.23 | 0.14 |
| 4 | 0.14 | 0.11 | 1.173 | 4.71 | 0.188 | 3.51 | 0.183 | 0.15 | 0.019 | 1.2 | 0.25 |
| 5 | 0.14 | 0.1 | 1.21 | 5.1 | 0.186 | 3.92 | 0.187 | 0.158 | 0.014 | 1.18 | 0.29 |
| 6 | 0.14 | 0.09 | 1.25 | 5.52 | 0.198 | 4.37 | 0.2 | 0.16 | 0.019 | 1.15 | 0.36 |
| 7 | 0.14 | 0.08 | 1.29 | 5.86 | 0.21 | 4.76 | 0.213 | 0.162 | 0.024 | 1.1 | 0.39 |
| 8 | 0.14 | 0.07 | 1.33 | 6.2 | 0.22 | 5.13 | 0.223 | 0.165 | 0.0275 | 1.07 | 0.42 |
| 9 | 0.14 | 0.06 | 1.35 | 6.52 | 0.229 | 5.47 | 0.235 | 0.166 | 0.0345 | 1.05 | 0.46 |
| 10 | 0.14 | 0.05 | 1.38 | 6.77 | 0.236 | 5.8 | 0.251 | 0.17 | 0.033 | 0.97 | 0.5 |
| 11 | 0.14 | 0.04 | 1.42 | 7.05 | 0.248 | 6.14 | 0.26 | 0.171 | 0.0385 | 0.91 | 0.54 |
| 12 | 0.14 | 0.03 | 1.43 | 7.36 | 0.259 | 6.44 | 0.254 | 0.182 | 0.0385 | 0.92 | 0.57 |
| 13 | 0.14 | 0.02 | 1.47 | 7.65 | 0.265 | 6.77 | 0.258 | 0.188 | 0.0385 | 0.88 | 0.61 |
| 14 | 0.14 | 0.01 | 1.5 | 7.88 | 0.275 | 6.93 | 0.26 | 0.2 | 0.0375 | 0.95 | 0.64 |
| 15 | 0.14 | 0 | 1.52 | 8.2 | 0.275 | 7.1 | 0.26 | 0.21 | 0.0325 | 1.1 | 0.68 |
| 16 | 0.14 | 0 | 1.57 | 8.2 | 0.275 | 7.4 | 0.26 | 0.22 | 0.0275 | 0.8 | 0.75 |
| 17 | 0.14 | 0 | 1.66 | 8.05 | 0.275 | 7.4 | 0.285 | 0.23 | 0.0225 | 0.65 | 0.86 |

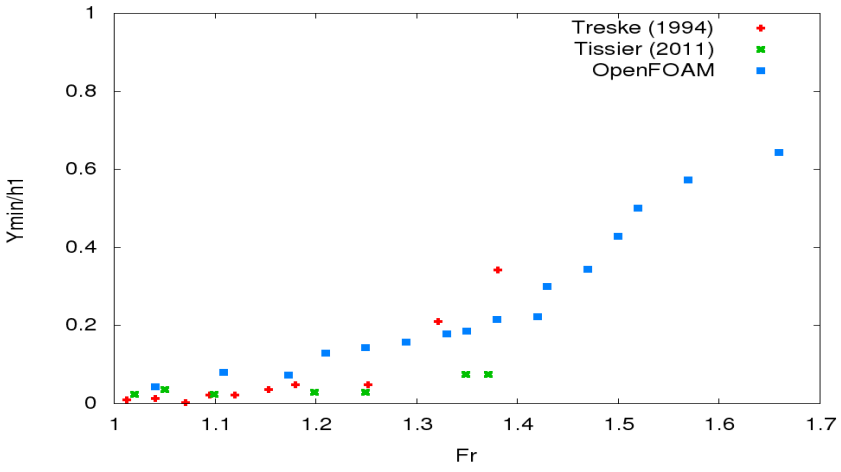


FIGURE 6 – Adimensional variable $Y_{min}/h1$ as a function of Froude number $Fr$.

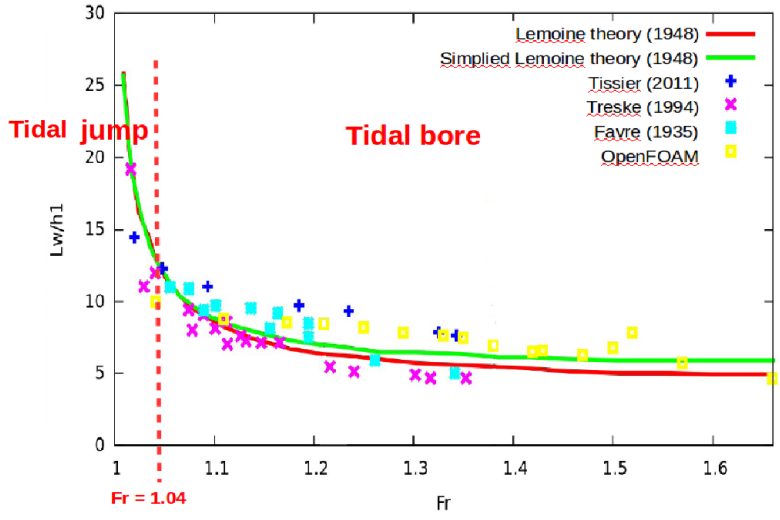


FIGURE 7 – Adimensional wavelength $L_w/h1$ as a function of Froude number $Fr$.

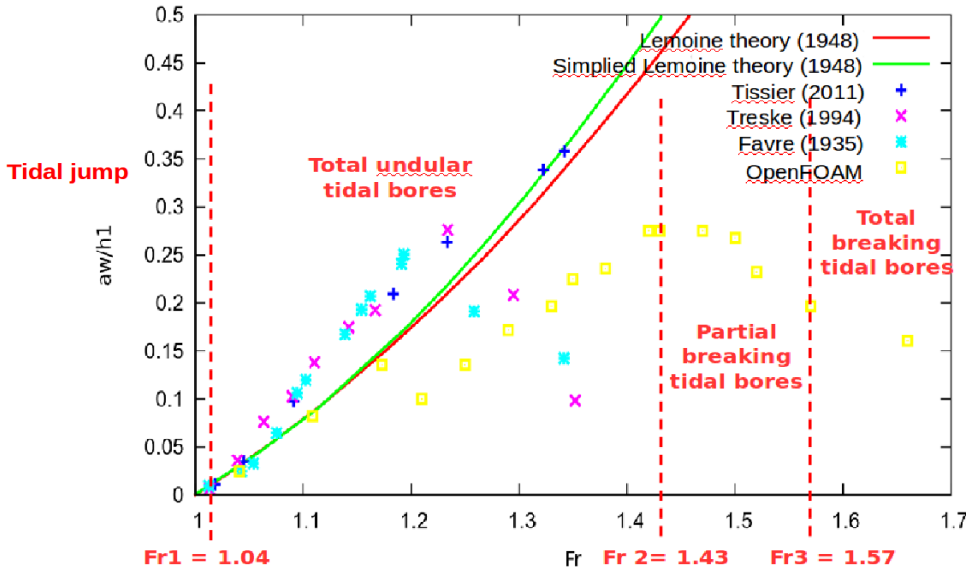


FIGURE 8 – Adimensional wave amplitude $a_w/h1$ as a function of Froude number $Fr$.

To confirm the values of $Fr_2$ and $Fr_3$, the variation rate of the elevation of free surface is studied. In Figure 9, the time evolution of this physical quantity was drawn in the two extreme cases, breaking tidal bore (a) and undular tidal bore (b). If the tidal bore is undular, the time derivative $dh/dt$ of the elevation of free surface is defined. If the tidal bore is breaking, the time derivative $dh/dt$ of the elevation of free surface is undefined and strong oscillations appear. After the analysis of all numerical simulations obtained with OpenFOAM, $Fr_2$ = 1.43 and $Fr_3$ = 1.57 are confirmed.

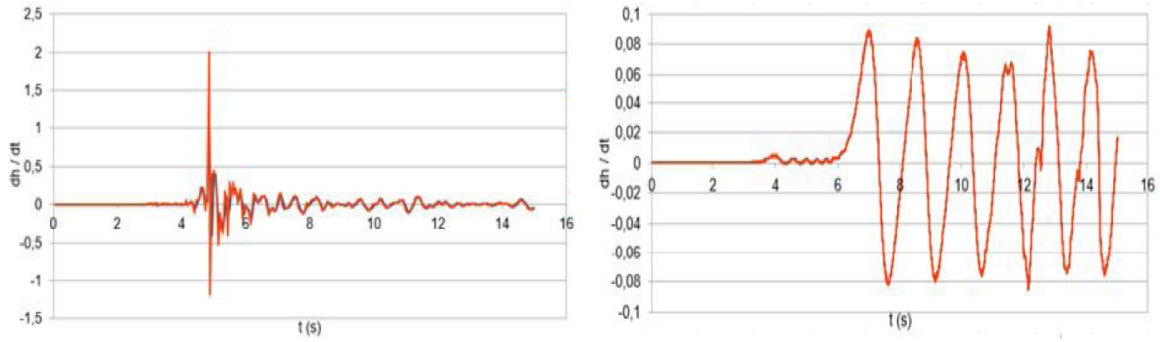


(a) (b)

FIGURE 9 – Time derivative of the elevation of free surface $dh/dt$ as a function of time $t$ for a breaking tidal bore (a) and an undular tidal bore (b).

## Transport analysis

In the case of undular tidal bores, the trajectory of sediment particles has been estimated to establish the relation between the parameters of the modified Chen's model, $\beta_1$, $\beta_2$ and $\beta_3$, and the Froude number $Fr$. Figure 10(a) shows the trajectory of a sediment particle with or without the effect of gravity. By subtracting the contribution of the settling velocity $w_s$ to the complete trajectory, the new trajectory is not affected by gravity. Figure 10(b) shows the trajectory of a sediment particle obtained with the modified Chen's model considering the effect of elevation (Eq. 9 and 10). Figure 10(c) shows the trajectory of a sediment particle obtained with the modified Chen's model considering all the mechanisms, gravity, elevation and attenuation. Figures 11(a), (b) and (c) show the numerical values of three parameters of the modified Chen's model, $\beta_1$, $\beta_2$ and $\beta_3$, as functions of Froude number $Fr$. The standard method of least squares has been used in order to obtain the best fitting of curves of three parameters, $\beta_1$, $\beta_2$ and $\beta_3$ :

$$y = -0.4085x + 0.7774 \quad \text{for} \quad \beta_1 \tag{14}$$

$$y = 17.438x - 17.496 \quad \text{for} \quad \beta_2 \tag{15}$$

$$y = 2.7439x - 3.1287 \quad \text{for} \quad \beta_3 \tag{16}$$

The least squares fits have been plotted in Figures 11(a), (b) and (c). The relation between the three parameters and the Froude number $Fr$ is linear. It may be explained by the low level of turbulence of undular tidal bores. The flow induced by undular tidal bores is not complex. This physical phenomenon is quasi-linear. Thus the theory of wave - current interactions is applicable. Then, the Chen's model can be adapted to the study of undular tidal bores. The parameter $\beta_1$ decreases when the Froude number $Fr$ increases (see Fig. 11(a)). The decrease of $\beta_1$ means a decrease of the velocity of the tidal bore front. The passage from undular tidal bores to breaking tidal bores induces a slowing of the passage of tidal bores. The two other parameters, $\beta_2$ and $\beta_3$, increase with the Froude number $Fr$ (see Fig. 11(b) and Fig. 11(c)). The parameter $\beta_2$ simulates the elevation of free surface generated by the passage of undular tidal bores. The increasing of Froude number $Fr$ induces an increase of this elevation. The flow of tidal bores, being more turbulent, has more energy for producing a more important elevation of free surface. The parameter $\beta_3$ simulates the attenuation of the wave train following the tidal bore front. The increase of Froude number $Fr$ induces an increase of this attenuation. The wave train disappears progressively with the Froude number $Fr$. The breaking tidal bores don't feature this wave train.

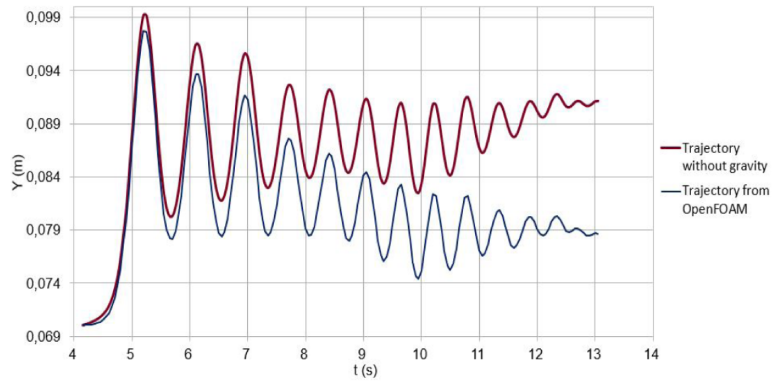


(a)

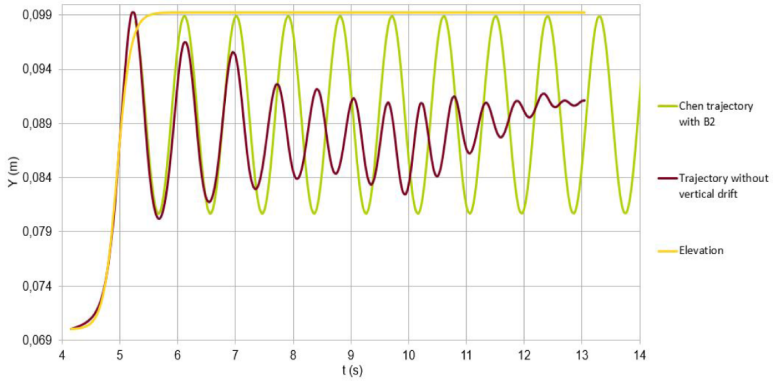


(b)

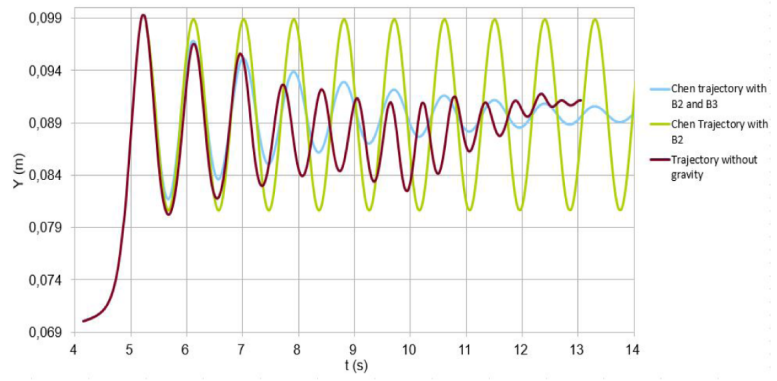


(c)

FIGURE 10 – Trajectory of a sediment particle induced by three effects : (a) gravity, (b) elevation and (c) gravity, elevation and attenuation.

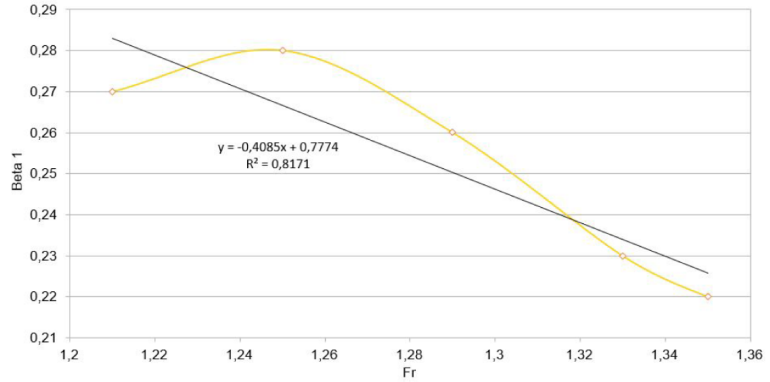


(a)

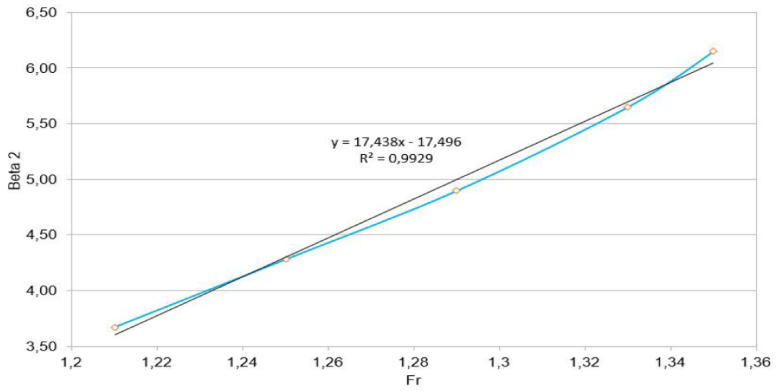


(b)

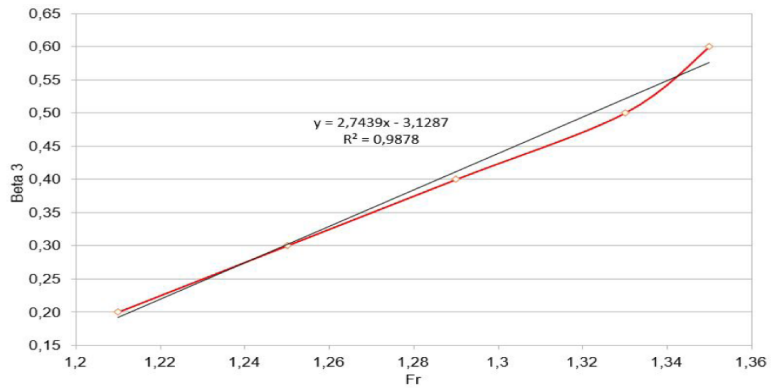


(c)

FIGURE 11 – Parameters of the modified Chen's model, $\beta_1$ (a), $\beta_2$ (b) and $\beta_3$ (c), as functions of the Froude number $Fr$ in the case of undular tidal bores.

# Conclusions

The Froude number $Fr$ is associated to the characterization of tidal bores, especially the description of free surface. The validation of numerical simulations obtained with OpenFOAM was based on the analysis of the shape of free surface for each configuration of the gate closing. This validation was checked with the good agreement between the numerical results obtained with OpenFOAM and the theoretical results obtained with the Lemoine's theory. The analysis of the shape of free surface has also allowed to define three transitions : tidal jumps / undular tidal bores, undular tidal bores / partial breaking tidal bores, and partial breaking tidal bores / total breaking tidal bores. The formation of undular tidal bores is established from $Fr_1$ = 1.04. The partial breaking tidal bores appear from $Fr_2$ = 1.43. They

become total breaking tidal bores from $Fr_3$ = 1.57.

To give a description of sediment particle trajectories under undular tidal bores, three modifications have been proposed to the Chen's model, based on the theory of wave - current interactions. Three parameters, $\beta_1$, $\beta_2$ and $\beta_3$ have been introduced. The relation between these three parameters and the Froude number $Fr$ is linear. $\beta_1$, related to the front celerity, decreases when $Fr$ increases. The undular tidal bores move faster than the breaking tidal bores. $\beta_2$ and $\beta_3$, related to the elevation and attenuation respectively, increase when $Fr$ increases. The undulations disappear progressively with $Fr$. The energy is dissipated because of the turbulence of breaking tidal bores.

# Références


[1] A. Berchet, Modélisation par des méthodes lagrangiennes du transport sédimentaire induit par les mascarets, Thèse, Université de Poitiers, 2014.

[2] H. Chanson, Environmental, ecological and cultural impacts of tidal bores, benaks, bonos and burros, International Workshop on Environmental Hydraulics Theoretical, Experimental and Computational Solutions, IWEH, Valencia, 2009.

[3] H. Chanson, Mixing and dispersion in tidal bores : A review, Proc. Intl Conf. on Estuaries & Coast, ICEC, Hangzhou, China, 2003.

[4] H. Chanson and K.K. Tan, Dispersion of fish eggs under undular and breaking tidal bores, FDMP, 7 (2011) 403-418.

[5] Y.-Y. Chen, H.-C. Hsu and H.-H. Wung, Particle trajectories beneath wave-current interaction in a two-dimensional field, Nonlin. Processes Geophys, 19 (2012) 185-197.

[6] H. Favre, Étude théorique et expérimentale des ondes de translation dans les canaux découverts, Paris : Dunod, 1935.

[7] L. Furgerot, Propriétés hydrodynamiques du mascaret et de son influence sur la dynamique sédimentaire. Une approche couplée en canal et in situ (estuaire de la Sée, Baie du Mont Saint-Michel), Thése, University of Caen, France, 2014.

[8] L. Furgerot, D. Mouazé, B. Tessier, L. Perez, S. Haquin, P. Weill and A. Crave, Sediment transport induced by tidal bores. An estimation from suspended matter measurements in the Sée River (Mont-Saint-Michel Bay, northwestern France), Comptes Rendus Geoscience, 348 (2016) 432-441.

[9] H. Jing, P.C. Hong, K. C. Ping, Z. Jian, and C.Gang, Experimental hydrodynamic study of the Qiantang River tidal bore, Journal of Hydrodynamics, 25(3) (2013) 481-490.

[10] N. Khezri, Modelling turbulent mixing and sediment process beneath tidal bores : physical and numerical investigations, PhD Thesis, University of Queensland, 2013.

[11] R. Lemoine, Sur les ondes positives de translation dans les canaux et sur le ressaut ondulé de faible amplitude, Houille Blance, (1948) 183-185.

[12] OpenFOAM, The open source cfd toolbox, User Guide, Version 3.0.1, OpenCFD Ltd., www.opencfd.co.uk/openfoam/, 2015.

[13] B. Simon, Effects of tidal bores on turbulent mixing : a numerical and physical study in positive surges. Thèse, Université Bordeaux and University of Queensland, 2013.

[14] M. Tissier, Étude numérique de la transformation des vagues en zone littorale, de la zone de levée aux zones de surf et de jet de river. Thèse, University of Bordeaux, 2011.

[15] A. Treske, Undular bores (Favre-waves) in open channels-Experimental studies, 32 (1994) 355-370.